Rita E. Mirza,[1] Milie M. Fang,[1] Eileen M. Weinheimer-Haus,[1,2] William J. Ennis,[2,3] and Timothy J. Koh[1,2]

# Sustained Inflammasome Activity in Macrophages Impairs Wound Healing in Type 2 Diabetic Humans and Mice

**The hypothesis of this study was that sustained activity of the Nod-like receptor protein (NLRP)-3 inflammasome in wounds of diabetic humans and mice contributes to the persistent inflammatory response and impaired healing characteristic of these wounds. Macrophages (Mp) isolated from wounds on diabetic humans and *db*/*db* mice exhibited sustained inflammasome activity associated with low level of expression of endogenous inflammasome inhibitors. Soluble factors in the biochemical milieu of these wounds are sufficient to activate the inflammasome, as wound-conditioned medium activates caspase-1 and induces release of interleukin (IL)-1β and IL-18 in cultured Mp via a reactive oxygen species–mediated pathway. Importantly, inhibiting inflammasome activity in wounds of *db*/*db* mice using topical application of pharmacological inhibitors improved healing of these wounds, induced a switch from proinflammatory to healing-associated Mp phenotypes, and increased levels of prohealing growth factors. Furthermore, data generated from bone marrow–transfer experiments from NLRP-3 or caspase-1 knockout to *db*/*db* mice indicated that blocking inflammasome activity in bone marrow cells is sufficient to improve healing. Our findings indicate that sustained inflammasome activity in wound Mp contributes to impaired early healing responses of diabetic wounds and that the inflammasome may represent a new therapeutic target for improving healing in diabetic individuals.**

*Diabetes 2014;63:1103–1114 | DOI: 10.2337/db13-0927*

Tissue repair involves overlapping phases of hemostasis, inflammation, proliferation, and remodeling (1). Diabetes can disrupt the timely progression through each phase of healing through its effects on many different cell types and molecular effectors (2). Macrophages (Mp) are involved in each phase of healing and are thought to play an important role in the repair of a variety of tissues (3–7). Thus, diabetes-induced disruptions in Mp function might be expected to impair healing.

Mp promote tissue repair by killing pathogens, clearing damaged tissue, and producing growth factors that induce angiogenesis, collagen deposition, and wound closure (4,8–11). During impaired healing associated with diabetes, wounds exhibit prolonged accumulation of Mp associated with elevated levels of proinflammatory cytokines and proteases and reduced levels of various growth factors (2,12,13). We recently demonstrated that Mp exhibit a sustained proinflammatory phenotype in wounds of diabetic mice (14) and that the persistence of the proinflammatory Mp phenotype appears to be

[1]Department of Kinesiology and Nutrition, University of Illinois at Chicago, Chicago, IL
[2]Center for Tissue Repair and Regeneration, University of Illinois at Chicago, Chicago, IL
[3]Department of Surgery, University of Illinois at Chicago, Chicago, IL

Corresponding author: Timothy J. Koh, tjkoh@uic.edu.

Received 13 June 2013 and accepted 31 October 2013.

This article contains Supplementary Data online at http://diabetes.diabetesjournals.org/lookup/suppl/doi:10.2337/db13-0927/-/DC1.

mediated at least in part by the proinflammatory cytokine interleukin (IL)-1β (15). However, much remains to be learned about the dysregulation of Mp in diabetic wounds.

Proinflammatory danger signals induce activity of a multiprotein complex called the Nod-like receptor protein (NLRP)-3 inflammasome (16–18). During inflammasome activation, the proform of caspase-1 is recruited to the NLRP-3 complex and cleaved to produce active caspase-1, which then cleaves and activates the potent proinflammatory cytokines IL-1β and IL-18. Elevated levels of IL-1β have been found in wounds of diabetic humans and mice (12,15,19,20), consistent with increased inflammasome activity. Since IL-1β, in turn, is known to induce a proinflammatory Mp phenotype (15,21), the NLRP-3 inflammasome may be part of a positive feedback loop that sustains inflammation in chronic wounds and contributes to impaired healing. Thus, the central hypothesis of this study is that sustained activity of the inflammasome in diabetic wounds contributes to impaired early healing responses of these wounds.

## RESEARCH DESIGN AND METHODS

### Human Subjects

Five patients (2 male and 3 female) with chronic wounds provided informed consent. Patients were diagnosed with type 2 diabetes and had nonhealing wounds on the sacral region or the lower limb lasting at least 3 months. During a sharp debridement, biopsies were taken from tissue located near the center of the wound. All procedures involving human subjects were approved by the institutional review board at the University of Illinois at Chicago according to Declaration of Helsinki principles.

### Animals

Diabetic *db/db* mice, nondiabetic *db*/+ controls, and C57Bl/6 wild-type controls were obtained from The Jackson Laboratory. Breeding pairs of NLRP-3 knockout mice were provided by Genentech, and caspase-1 knockout mice were provided by Drs. Mihai Netea and Leo Joosten, Radboud University Nijmegen Medical Center. Experiments were performed on 12- to 16-week-old mice. All procedures involving animals were approved by the animal care committee at the University of Illinois at Chicago.

### Excisional Wounding and Treatment

Mice were subjected to excisional wounding with an 8-mm biopsy punch as described previously (14,15). Wounds were treated with the caspase-1 inhibitor Tyr-Val-Ala-Asp (YVAD) or the inflammasome inhibitor glyburide as indicated; treatment was initiated 3 days postinjury to allow the initial inflammatory response to proceed normally. Ac-YVAD-cmk (20 μmol/L; Cayman Chemical) and glyburide (200 μmol/L; InvivoGen) were applied topically to wounds every other day in F-127 pluronic gel (50 μL of a 25% gel in saline) (22,23). Controls were treated with DMSO vehicle-loaded gel.

### Bone Marrow Transfer

Bone marrow–recipient mice (8- to 10-week-old *db/db* mice) were subjected to lethal irradiation by 2 doses of 5 Gray at 1.02 Gray/min with 3 h between doses. Bone marrow cells were collected from donor 8- to 10-week-old C57Bl/6 wild-type, caspase-1–null, and NLRP-3–null mice and injected retro-orbitally ($5 \times 10^6$ cells per mouse in 200 μL saline) into recipient mice at 1 day after lethal irradiation. Mice were allowed to recover for 30 days and then subjected to excisional wounding. Engraftment was verified in preliminary experiments using congenic mice and was found to be >85% by flow cytometry.

### Cell Isolation

Cells were dissociated from human chronic wound biopsies and mouse excisional wounds using an enzymatic digest (14). Neutrophils, T cells, and B cells were marked for depletion by incubating cells for 15 min with fluorescein isothiocyanate (FITC)-conjugated anti-Ly6G (1A8), anti-CD3 (17A2), and anti-CD19 (6D5) for mouse cells and FITC-conjugated anti-CD15 (HI98), anti-CD3 (UCHT1), and anti-CD19 (HIB19) for human cells (1:10; all from Biolegend) and then depleted from the total cell population using anti-FITC magnetic beads (Miltenyi Biotec). Cells of the monocyte/Mp lineage were then isolated using CD11b magnetic beads.

### RNA Analysis

Total RNA was isolated from human or mouse cells using the RNeasy kit (Qiagen). cDNA was synthesized using the Thermoscript RT-PCR System (Invitrogen). Real-time PCR was performed using TaqMan Universal PCR Master Mix and TaqMan Gene Expression Assay primer/probe sets (Applied Biosystems). Relative gene expression was determined using the $2^{-\Delta\Delta CT}$ method, with GAPDH as the endogenous control gene.

### Flow Cytometry

Cells were dissociated from mouse wounds, and neutrophils, T cells, and B cells were depleted by magnetic sorting as described above. The remaining cells were stained using phycoerythrin-conjugated anti-CD11b (clone M1/70, diluted 1:10), and active caspase-1 was labeled using the FLICA detection reagent (Immunochemistry Technologies). Mp containing active caspase-1 were identified as $CD11b^+FLICA^+$ cells.

### Immunofluorescence

Cryosections (10-μm thick) were cut from human chronic wound biopsies, fixed in cold acetone and blocked with buffer containing 3% BSA. Sections were then incubated overnight with primary antibodies against CD68 (clone Y1/82A, 1:100; Biolegend) and caspase-1 (Millipore). Sections were then incubated with FITC- and tetramethylrhodamine isothiocyanate-conjugated isotype-specific secondary antibodies (1:200; Invitrogen). Negative

controls included nonstained slides and isotype-specific control antibodies (IgG1 and IgG2b; Biolegend) along with secondary antibodies. Digital images were obtained using a Nikon Instruments Eclipse 80i microscope with a ×20/0.75 objective, a DS-Fi1 digital camera, and NIS Elements software.

### Wound-Healing Assays

For mouse wounds, healing was assessed on day 10 postinjury using our previously published assays of granulation tissue formation and re-epithelialization using hematoxylin-eosin–stained cryosections (4,14). In addition, angiogenesis, *myo*-fibroblast accumulation, and collagen deposition were measured in CD31-, α-smooth–muscle actin–, and Trichrome-stained cryosections, respectively (4,14). For all assays, digital images were obtained using a Nikon Instruments 80i microscope and DS-QI1 digital camera and analyzed using NIS Elements image analysis software.

### Cell Culture

For generation of cultures of human Mp, peripheral blood mononuclear cells from normal volunteers (ZenBio) were plated in RPMI supplemented with 10% FBS, 2 mmol/L L-glutamine, 1% penicillin/streptomycin, and 20 ng/mL recombinant human M-CSF (Peprotech). After 7 days in culture, cells were stimulated for 18 h with interferon-γ (IFN-γ) and tumor necrosis factor (TNF)-α (20 ng/mL each; Peprotech) or 20% human wound-conditioned medium along with DMSO vehicle, YVAD, or glyburide. Wound-conditioned medium was generated by incubating biopsies in Dulbecco's modified Eagle's medium plus 10% FBS (1 mL/100 mg tissue) for 2 h at 37°C.

Bone marrow–derived mouse Mp were cultured from wild-type C57Bl/6 mice and IL1R1, NLRP-3, and caspase-1 knockout mice as previously described (24). Mp were stimulated for 18 h with IFN-γ and TNF-α (20 ng/mL each; R&D Systems) or 20% mouse wound-conditioned medium with IL-1β blocking antibody, YVAD, glyburide, the antioxidant *N*-acetyl cysteine (NAC), or the NADPH oxidase inhibitor diphenyliodonium (DPI) or appropriate controls. (See figures for details.) Mouse wound–conditioned medium was generated by incubating excised wounds in Dulbecco's modified Eagle's medium plus 10% FBS (1 mL/100 mg tissue) for 2 h at 37°C.

For measurement of reactive oxygen species (ROS), cells were incubated in 5 μmol/L 5(6)-carboxy-2′,7′-dichlorofluorescein diacetate (DCF-DA; Invitrogen) for 10 min at 37°C and stimulated with wound-conditioned medium with 25 mmol/L NAC, 25 μmol/L DPI, or vehicle for 1 h at 37°C. Controls were loaded with DCF-DA but not treated with conditioned medium. Median DCF fluorescence was measured by flow cytometry (Accuri C6) and expressed relative to controls.

### ELISA

Mouse wounds were homogenized in cold PBS (10 μL PBS/mg wound tissue) supplemented with protease inhibitor cocktail (Sigma). Supernatants of wound homogenates or cell culture medium were used for ELISA for IL-1β, IL-6, IL-10, TGF-β1, TNF-α (eBioscience), IL-18 (MBL International), and IGF-1 (R&D Systems). When wound-conditioned medium was used as a cell culture supplement, cytokine release was measured as the difference between levels achieved in wells with cultured cells and levels in blank wells that contained identical medium composition but no cells.

### Statistics

Values are reported as means ± SD. Measurements of Mp gene expression, cytokine and growth factor levels, ROS production, re-epithelialization, granulation tissue thickness, Trichrome staining, and CD31-staining data were compared using ANOVA. ANOVA on ranks was used if data sets did not pass tests of normality and equal variance. The Student-Newman-Keuls post hoc test was used when ANOVAs demonstrated significance. Differences between groups were considered significant if $P \leq 0.05$.

## RESULTS

### Inflammasome Components in Mp From Chronic Diabetic Human Wounds

Subjects recruited for this study were obese and diabetic (Supplementary Table 1). Mp isolated from chronic wounds expressed high levels of inflammasome components NLRP-3 and caspase-1, and inflammasome targets IL-1β and IL-18, but only low levels of proteinase inhibitor-9 (PI-9) and caspase-12, which are negative regulators of inflammasome activity (Fig. 1*A*–*F*). Overall, expression of inflammasome components in chronic wound Mp was remarkably similar to that of blood-derived Mp stimulated with IFN-γ and TNF-α in vitro, with the striking exception of PI-9 and caspase-12, which were expressed at low levels in wound Mp. Immunofluorescent staining of chronic wound cryosections confirmed protein expression of the end effector of the inflammasome, caspase-1, in the majority of $CD68^+$ wound Mp (Fig. 1*G*–*I*).

### Sustained Inflammasome Activity in Mp From Diabetic Mouse Wounds

As expected, *db/db* mice were obese and diabetic (Supplementary Table 2). Mp expression and release of IL-1β and IL-18 was high on day 5 postinjury and then downregulated on day 10 postinjury in *db*/+ mice. In contrast, expression and release of these inflammasome targets were maintained at high levels on day 10 in *db/db* mice (Fig. 2*A*, *B*, *E*, and *F*). When different wound cell populations were compared, Mp were the dominant producers of IL-1β and IL-18 after wounding in both *db*/+ and *db/db* mice (Fig. 2*C* and *D*). These data indicate that inflammasome activity is downregulated as wound healing progresses in *db*/+ mice but is sustained at high levels in *db/db* mice.

High-level activation of caspase-1 was confirmed in *db/db* versus *db*/+ wound Mp by flow cytometry using

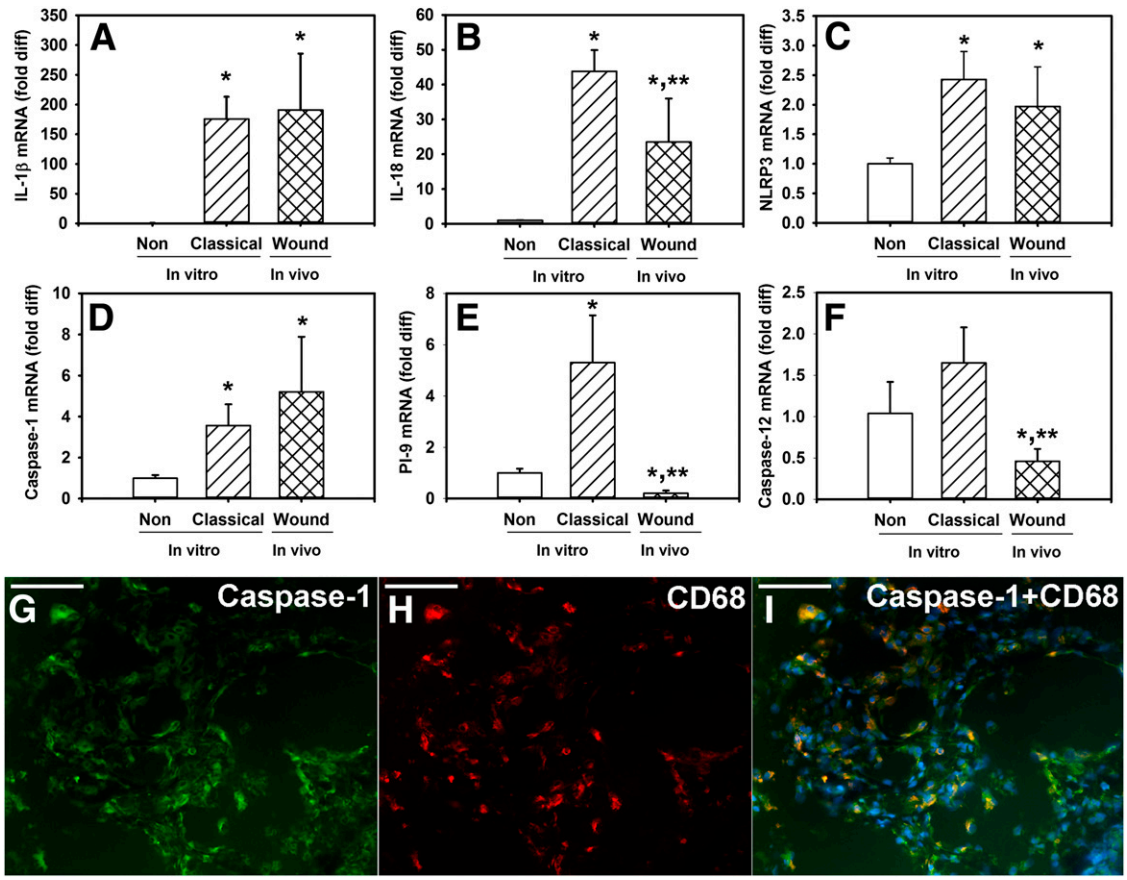


**Figure 1**—Mp from chronic wounds of diabetic patients express components of the NLRP-3 inflammasome. *A–F*: Mp isolated from chronic wound biopsies and expression of IL-1β, IL-18, NLRP-3, caspase-1, PI-9, and caspase-12 assessed by real-time PCR. For comparison, blood-derived Mp from healthy volunteers were either left nonstimulated (Non) or stimulated with TNF-α and IFN-γ (classical) and gene expression was assessed along wound Mp. *G–I*: Wound biopsy cryosections immunostained for caspase-1 and the Mp marker CD68; scale bar = 100 μm. For all graphs, bars = mean ± SD, $n = 5$. Data compared between groups using ANOVA on ranks. *Mean value significantly different from that for nonstimulated controls; **mean value significantly different from that for classically activated cells; $P < 0.05$. Diff, difference.

labeled YVAD that binds to active caspase-1 (Fig. 2*G* and *H*); active caspase-1 was detected in 4.8 ± 1.1% of *db*/+ wound Mp and in 9.9 ± 1.4% of *db/db* wound Mp (mean ± SD). Interestingly, although no difference was observed in Mp expression of NLRP-3 or caspase-1 on days 5 and 10 postinjury in either *db*/+ or *db/db* mice (Fig. 2*I* and *J*), expression of the inflammasome inhibitors PI-9 and caspase-12 was upregulated from day 5 to day 10 postinjury in *db*/+ mice (Fig. 2*K* and *L*), associated with the downregulation of inflammasome activity. In contrast, expression of these inflammasome inhibitors was maintained at low levels in *db/db* mice, associated with sustained high levels of inflammasome activity. These data indicate that, during wound healing, activity of the inflammasome may be regulated at least in part by expression of its endogenous inhibitors.

### Diabetic Wound Environment Is Sufficient to Upregulate Inflammasome Activity

To provide insight into whether soluble factors in the biochemical milieu of the wound can activate the inflammasome in both human and mouse Mp, we cultured nonactivated Mp with conditioned medium of wounds from diabetic individuals of each species. First, blood-derived Mp from normal human subjects were stimulated with chronic wound–conditioned medium from diabetic patients. Wound-conditioned medium increased release of IL-1β and IL-18 into the medium surrounding cultured Mp (Fig. 3*A* and *B*). Activation of the inflammasome was confirmed, as both the caspase-1 inhibitor YVAD and the inflammasome inhibitor glyburide reduced the conditioned medium–induced release of IL-1β and IL-18. Activation of caspase-1 was also assessed in conditioned medium–treated cells by flow cytometry (Fig. 3*C* and *D*); active caspase-1 was detected in 2.9 ± 0.7% of nonstimulated control cells and in 10.5 ± 1.3% of conditioned medium–stimulated cells.

Next, bone marrow–derived Mp from wild-type (C57Bl/6) mice were stimulated with conditioned medium of wounds from *db/db* mice. Wound-conditioned medium from *db/db* mice induced IL-1β and IL-18 release, and both YVAD and glyburide reduced cytokine

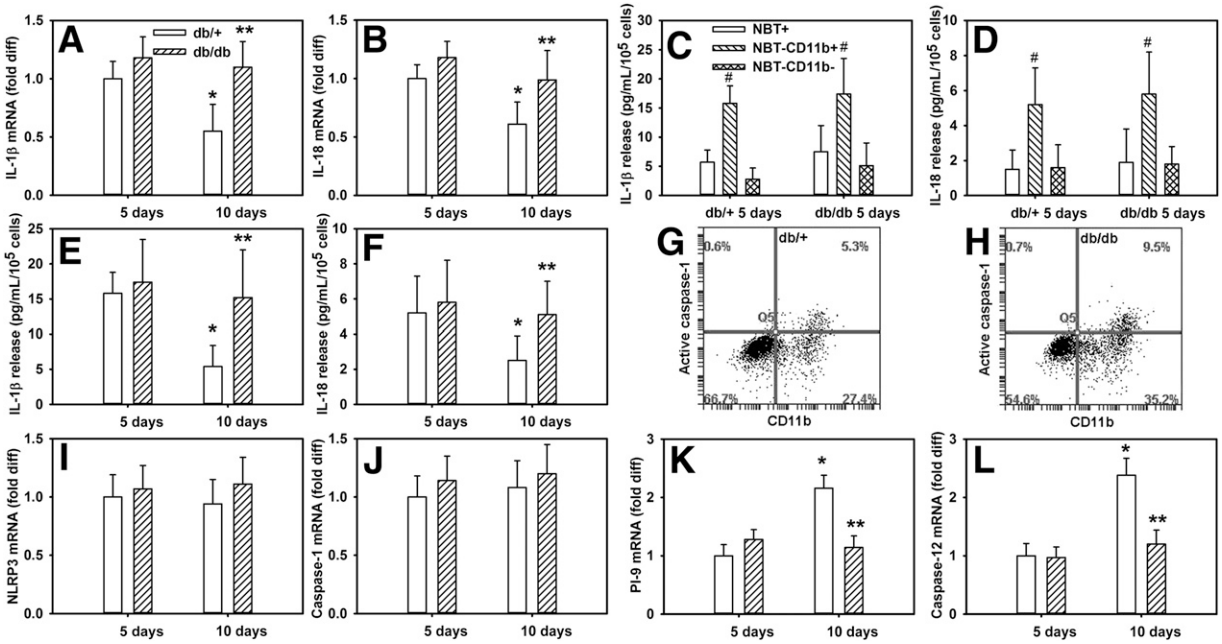


**Figure 2**—Mp exhibit sustained inflammasome activity in wounds of diabetic mice. *A* and *B*: Mp isolated from wounds of nondiabetic (*db*/+) and diabetic (*db*/*db*) mice on days 5 and 10 postinjury and expression of IL-1β and IL-18 assessed by real-time PCR. *C* and *D*: Neutrophils (Ly6G$^+$)/B cells (CD19$^+$)/T cells (CD3$^+$) (combined NBT$^+$ cells), Mp (NBT$^-$CD11b$^+$ cells), and remaining cells (NBT$^-$CD11b$^-$ cells) isolated from day 5 *db*/+ and *db*/*db* wounds and incubated overnight; release of IL-1β and IL-18 measured using ELISA. *E* and *F*: Mp (NBT$^-$CD11b$^+$ cells) isolated from day 5 and 10 *db*/+ and *db*/*db* wounds and incubated overnight; release of IL-1β and IL-18 measured using ELISA. *G* and *H*: Representative flow cytograms of active caspase-1 in Mp (NBT$^-$CD11b$^+$ cells) isolated from day 10 *db*/+ and *db*/*db* wounds. *I*-*L*: Mp isolated from *db*/+ and *db*/*db* wounds on days 5 and 10 postinjury and expression of NLRP-3, caspase-1, PI-9, and caspase-12 assessed by real-time PCR. For all graphs, bars = mean ± SD, $n$ = 6–8. Data compared between groups using ANOVA. *Mean value significantly different from that for same strain on day 5 postinjury; **mean value for *db*/*db* mice significantly different from that for *db*/+ mice at same time point; #mean value significantly different from those for other cell types; $P < 0.05$. Diff, difference.

release (Fig. 3*E* and *F*). As a control, we cultured Mp with conditioned medium from noninjured *db/db* skin samples and found that noninjured skin–conditioned medium did not induce IL-1β or IL-18 release from cultured Mp (data not shown). In addition, whereas *db/db* wound-conditioned medium induced IL-1β and IL-18 release from wild-type Mp, cytokine release was absent from NLRP-3 and caspase-1–null Mp (Fig. 3*G* and *H*). Thus, wound-conditioned medium–induced IL-1β and IL-18 release appears to be mediated by the NLRP-3 inflammasome.

### Blocking ROS Reduces Inflammasome Activity in Cultured Mp

Whereas a number of different danger signals, including ATP, uric acid crystals, cholesterol crystals, and glucose, can activate the inflammasome (16,17,25), a common downstream mediator may be increased production of ROS (25). To determine whether wound-conditioned medium induces ROS production from cultured Mp, we used the ROS-sensitive fluorescent dye DCF-DA. Conditioned medium from day 5 wounds of both *db*/+ and *db/db* mice increased DCF fluorescence in cultured Mp above medium-only controls (Fig. 4*A*). Conditioned medium from day 10 wounds of *db*/+ mice did not increase DCF fluorescence, but conditioned medium from *db/db* mice increased DCF fluorescence to a level similar to that of day 5 conditioned medium. Thus, ROS induction by wound-conditioned medium paralleled IL-1β and IL-18 production from cultured Mp. We next inhibited ROS production using the antioxidants NAC and DPI (Fig. 4*B*–*D*) and found that such treatment reduced IL-1β and IL-18 release. In total, these data indicate that the diabetic wound environment activates the inflammasome at least partly by increasing ROS production.

### Blocking IL-1β Activity Reduces Inflammasome Activity in Cultured Mp

Inflammasome activation is thought to be a two-step process in which the initial signal induces expression of IL-1β and IL-18 and a second stimulus induces cleavage of IL-1β and IL-18 (16,17,25). To determine whether IL-1β itself contributes to the initial signal in this process, we treated cultured Mp with day 10 *db/db* wound-conditioned medium and blocked IL-1β signaling with an IL-1β blocking antibody. Wound-conditioned medium upregulated expression and release of IL-1β and IL-18, and the IL-1β blocking antibody inhibited the induction and release of these cytokines (Fig. 5*A*, *B*, *G*, and *H*). Interestingly, wound-conditioned medium downregulated expression of NLRP-3, caspase-1, PI-9, and caspase-12, but the blocking antibody only inhibited the downregulation of PI-9 and caspase-12 (Fig. 5*C*–*F*).

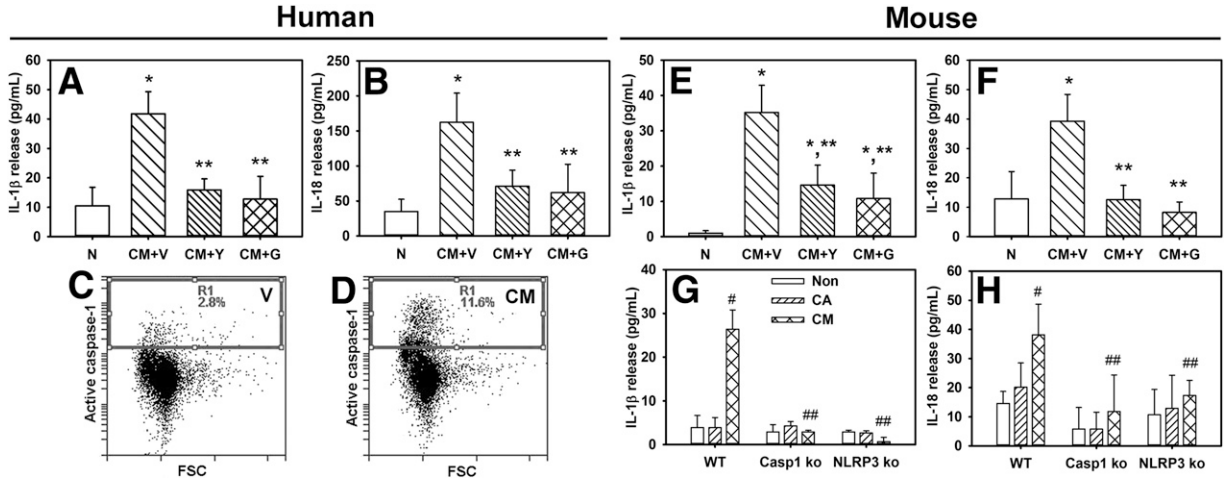


**Figure 3—**Wound-conditioned medium activates the inflammasome in both human and mouse Mp in vitro. *A* and *B*: Blood-derived Mp from healthy human volunteers either left nonstimulated (N) or stimulated with chronic wound–conditioned medium (CM) along with vehicle (V), the caspase-1 inhibitor YVAD (Y) (20 μmol/L), or the inflammasome inhibitor glyburide (G) (200 μmol/L) and release of IL-1β and IL-18 measured by ELISA. *C* and *D*: Representative flow cytograms of active caspase-1 in human blood–derived Mp, Mp either left nonstimulated or stimulated with chronic wound–conditioned medium. *E* and *F*: Bone marrow–derived Mp from wild-type (C57BL/6) mice either left nonstimulated or stimulated with day 10 *db/db* wound-conditioned medium along with vehicle or the same inhibitors as used for human Mp and release of IL-1β and IL-18 measured by ELISA. *G* and *H*: Bone marrow–derived Mp from wild-type (WT), caspase-1 (Casp1), and NLRP-3 knockout (ko) mice left nonstimulated (Non), stimulated with TNF-α and IFN-γ (20 ng/mL each) (CA), or stimulated with day 10 *db/db* wound-conditioned medium (CM). For all graphs, bars = mean ± SD, $n$ = 5–6 in two separate experiments. Data compared between groups using ANOVA on ranks. *Mean value significantly different from that for nonstimulated controls; **mean value significantly different from that for wound-conditioned medium + vehicle-treated cells; #mean value significantly different from that for nonstimulated controls; ##mean value significantly different from that for wound-conditioned medium–treated wild-type Mp; $P < 0.05$. FSC, forward scatter.

One should note that, in this experiment, the IL-1β blocking antibody may interfere with ELISA assessment of IL-1β release, but the measurement of IL-18 release should be reflective of inflammasome activity.

The IL-1β blocking antibody data were corroborated in experiments using Mp cultured from IL-1 receptor 1 (IL-1R1) knockout mice; compared with wild-type Mp, wound-conditioned medium–treated IL-1R1 knockout Mp exhibited blunted upregulation of IL-1β and IL-18 expression and release (Fig. 5*I*, *J*, *O*, and *P*) and blunted downregulation of PI-9 and caspase-12 (Fig. 5*M* and *N*). These data indicate that IL-1R1 knockout Mp are less sensitive to wound-conditioned medium–induced inflammasome activity than are wild-type Mp. Taken together, these data indicate that IL-1β in the diabetic wound environment may induce expression of IL-1β and IL-18 and contribute to sustained inflammasome activity in wound Mp.

### Blocking Inflammasome Activity Improves Healing in *db/db* Mice

To determine whether inhibiting inflammasome activity can improve healing of wounds in *db/db* mice, we applied the NLRP-3 inflammasome inhibitor glyburide or the irreversible caspase-1 inhibitor YVAD topically to wounds of *db/db* mice. Mice whose wounds were treated with glyburide or YVAD showed no change in body weight or blood glucose levels compared with vehicle-treated mice (Supplementary Table 2). Treatment with glyburide or YVAD accelerated re-epithelialization and increased granulation tissue formation (Fig. 6*A–D*) and glyburide but not YVAD treatment increased collagen deposition on day 10 postinjury (Fig. 6*E*). Whereas neither glyburide nor YVAD treatment influenced angiogenesis as assessed by CD31 labeling (Fig. 6*F*), both treatments led to increased α-smooth-muscle actin staining, indicating increased *myo*-fibroblasts (Supplementary Fig. 1).

As expected, treatment with either glyburide or YVAD reduced levels of IL-1β and IL-18 in wound homogenates (Fig. 6*G* and *H*), consistent with reduced activity of the NLRP-3 inflammasome and caspase-1. In addition, there were nonsignificant trends of decreased TNF-α and IL-6 in glyburide- and YVAD-treated wounds (Fig. 6*I* and *J*). In contrast, wound levels of IGF-1 and TGF-β were increased both by glyburide and by YVAD treatment (Fig. 6*K* and *L*), indicating a more prohealing wound environment.

To determine whether the change in wound environment and improved healing were associated with a change in Mp phenotype, we isolated Mp from wounds treated with DMSO vehicle or glyburide. Compared with Mp from DMSO-treated wounds, Mp from glyburide-treated wounds exhibited lower-level expression of IL-1β, IL-18, and TNF-α (Fig. 6*O–Q*), although expression of IL-6 was increased (Fig. 6*R*), as was expression of IGF-1, TGF-β, IL-10, and CD206 (Fig. 6*S–V*). (Note that changes in Mp phenotype with YVAD treatment were not measured.) These data indicate that blocking inflammasome

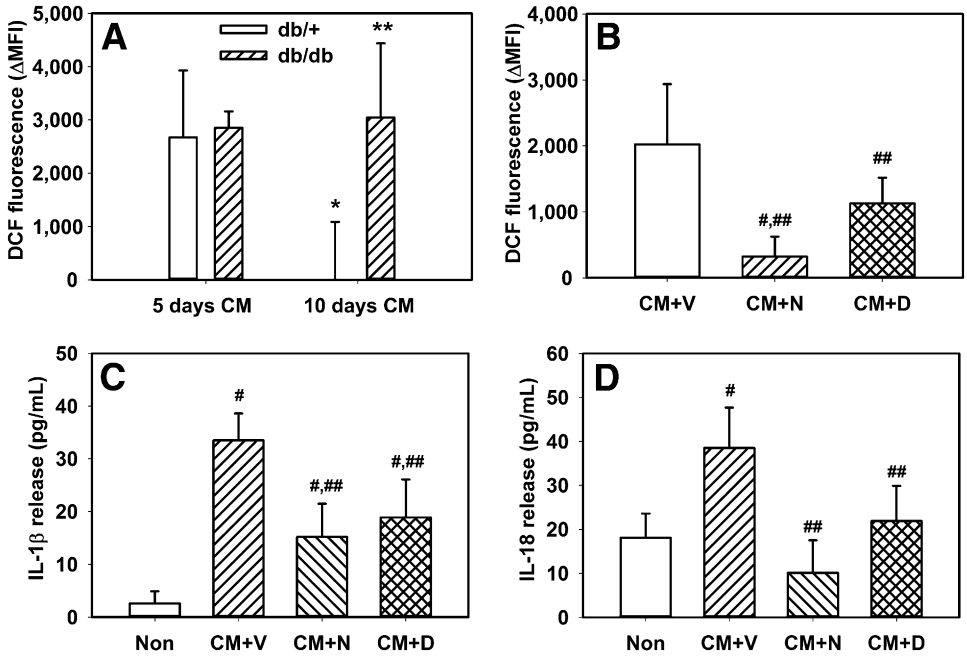


**Figure 4—**ROS inhibitors block conditioned medium–induced inflammasome activity in cultured Mp. *A*: Bone marrow–derived Mp from wild-type mice were cultured with wound-conditioned medium (CM) of day 5 or 10 wounds from nondiabetic *db*/+ or diabetic *db*/*db* mice, and ROS generation was measured using DCF-DA and flow cytometry. DCF fluorescence measured as the difference in median fluorescence intensity (MFI) between wound-conditioned medium–treated cells and nonstimulated controls. *B–D*: Bone marrow–derived Mp from wild-type mice treated with day 10 *db*/*db* wound-conditioned medium along with vehicle (V), NAC (N) (25 mmol/L), or DPI (D) (25 μmol/L); ROS measured as change in median fluorescence intensity and IL-1β, and IL-18 release measured using ELISA. For all graphs, bars = mean ± SD, $n = 6$ in two independent experiments. Data compared between groups using ANOVA on ranks. *Mean value significantly different from that for wound-conditioned medium of same strain on day 5 postinjury; **mean value for *db*/*db* CM significantly different from that for *db*/+ wound-conditioned medium at same time point; #mean value significantly different from that for nonstimulated controls; ##mean value significantly different from that for wound-conditioned medium + vehicle-treated samples; $P < 0.05$.

activity downregulated Mp expression of proinflammatory cytokines measured and upregulated expression of prohealing factors, which, in turn, was associated with a more prohealing wound environment and improved healing in *db/db* mice.

### Bone Marrow Transfer Between NLRP-3–Null and *db*/*db* Mice Improves Healing in *db*/*db* Mice

To more specifically target the inflammasome in Mp, we used bone marrow transfer to determine the role of bone marrow cell–derived inflammasome activity in impaired healing of wounds in diabetic mice. Bone marrow transfer from wild-type to *db/db* mice resulted in wound healing that was similar to *db/db* mice that had not received bone marrow transfer (compare Fig. 7*A–D* with Fig. 6*A–D* and refs. 14,15), indicating that impaired healing is not a result of intrinsic defects in *db/db* Mp. In contrast, transfer of NLRP-3– or caspase-1–null bone marrow resulted in accelerated re-epithelialization and increased granulation tissue formation, mimicking the effects of the inflammasome inhibitors (Fig. 7*A–D*). In addition, transfer of NLRP-3–null but not caspase-1–null bone marrow resulted in increased collagen deposition (Fig. 7*E*). Although transfer of bone marrow from either NLRP-3– or caspase-1–null mice did not influence angiogenesis (Fig. 7*F*), in both cases, α-smooth-muscle actin staining was increased (Supplementary Fig. 2).

Furthermore, bone marrow transfer from NLRP-3–null or caspase-1–null mice to *db/db* mice resulted in reduced levels of IL-1β and IL-18 in wound homogenates (Fig. 7*G* and *H*), indicating that bone marrow–derived NLRP-3 inflammasome produces the majority of IL-1β and IL-18 in these wounds. These bone marrow transfers also reduced levels of TNF-α and IL-6 (Fig. 7*I* and *J*), indicating additional downregulation of the proinflammatory wound environment. In contrast, wound levels of IGF-1 and TGF-β were increased by transfer of both NLRP-3– and capase-1–null bone marrow (Fig. 7*K* and *L*), indicating the induction of a more prohealing wound environment.

## DISCUSSION

Chronic wounds are typically associated with a persistent inflammatory response that involves accumulation of Mp (19,26–28); however, little is known about the regulation and function of Mp in nonhealing wounds. We and others have observed a persistent proinflammatory wound Mp phenotype in diabetic humans and mice (14,29) and in chronic venous ulcers (30). The major novel finding of this study is that the NLRP-3

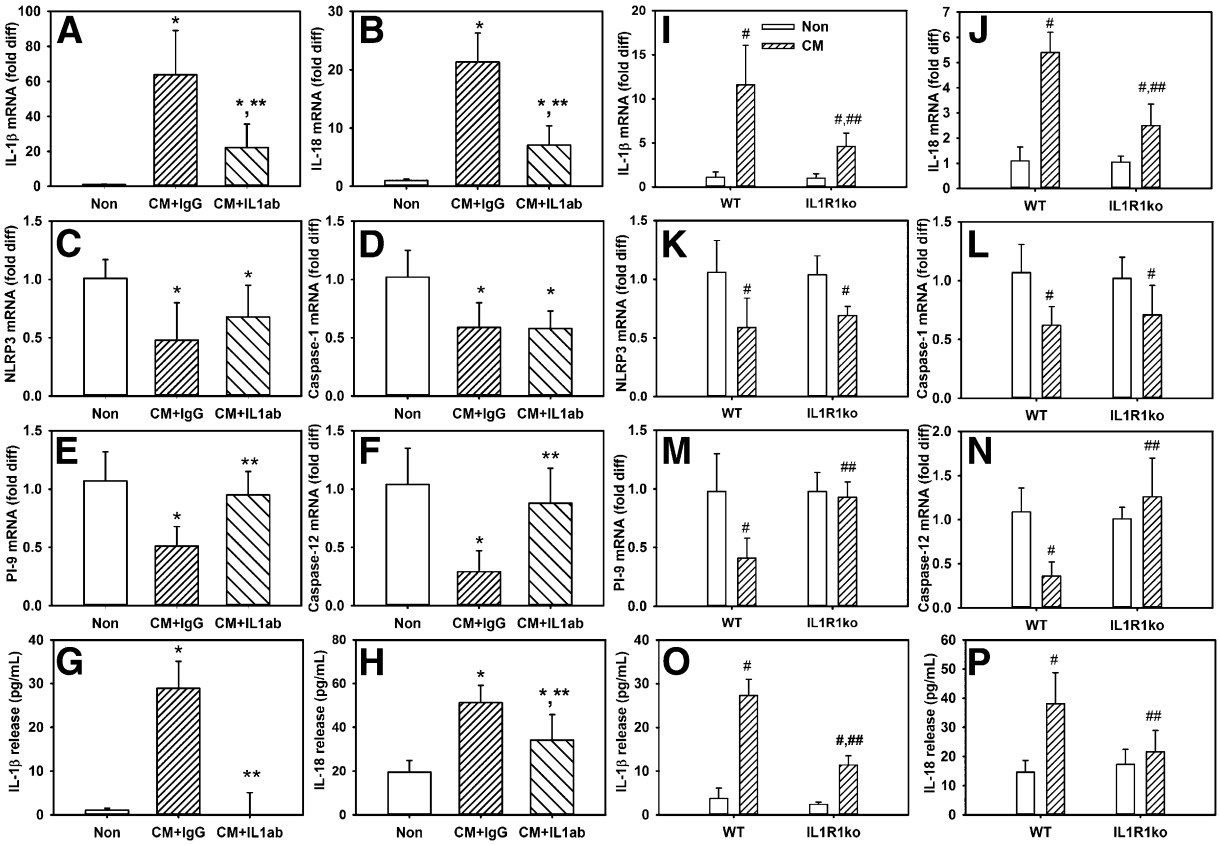


**Figure 5—**Blocking IL-1β signaling blunts conditioned medium–induced inflammasome activity in vitro. *A–F*: Bone marrow–derived Mp from wild-type (WT) mice either left nonstimulated (Non) or stimulated with day 10 *db/db* wound-conditioned medium (CM) along with control IgG or IL-1β blocking antibody (IL1ab), and expression of IL-1β, IL-18, PI-9, and caspase-12 measured by real-time PCR. *G* and *H*: Bone marrow–derived Mp from wild-type mice either left nonstimulated or treated with day 10 *db/db* wound CM along with control IgG or IL-1β blocking antibody and IL-1β and IL-18 release measured using ELISA. *I–N*: Bone marrow–derived Mp from WT and IL-1R1 knockout (ko) mice stimulated with day 10 *db/db* wound CM and expression of IL-1β, IL-18, PI-9, and caspase-12 measured by real-time PCR. *O* and *P*: Bone marrow–derived Mp from WT and IL-1R1ko mice stimulated with day 10 *db/db* CM and IL-1β and IL-18 release measured using ELISA. For all graphs, bars = mean ± SD, $n$ = 5–6 in two independent experiments. Data compared between groups using ANOVA on ranks. *Mean value significantly different from that for nonstimulated controls; **mean value significantly different from that for wound-conditioned medium + IgG-treated samples; #mean value significantly different from that for nonstimulated controls; ##mean value significantly different from that for wound-conditioned medium–treated wild-type Mp at same time point; $P < 0.05$. Diff, difference.

inflammasome is a key regulatory pathway in the chronic inflammatory response in wounds of diabetic humans and mice. In vitro studies indicated that the diabetic wound environment is sufficient to activate the inflammasome in cultured Mp via an ROS-mediated pathway and that its downstream target IL-1β participates in a proinflammatory positive-feedback loop that contributes to the persistent inflammatory response (Fig. 8). Importantly, inhibiting the inflammasome in vivo, either using topical application of pharmacological inhibitors or via bone marrow transfer from NLRP-3– or caspase-1–null mice to *db/db* mice, promotes the early healing response in part by downregulating the proinflammatory phenotype characteristic of Mp in diabetic wounds and increasing production of prohealing factors.

The NLRP-3 inflammasome plays a role in the pathophysiology of many inflammatory diseases, including obesity, insulin resistance, and diabetes (21,31–35). Although previous studies have demonstrated that platelet-derived growth factor, fibroblast growth factor, vascular endothelial growth factor (VEGF), or erythropoietin can improve healing in diabetic mice (13,36,37), our data indicate that targeting the inflammasome may provide a novel target for improving healing in diabetic patients. Glyburide is a commonly used sulfonylurea drug for the treatment of type 2 diabetes and was recently shown to inhibit the NLRP-3 inflammasome through a mechanism that appears to be different from that involved in its ability to promote insulin secretion from pancreatic β-cells (38). In our studies, topical glyburide improved wound healing in diabetic mice, and thus this U.S. Food and Drug Administration–approved drug may represent a convenient and effective therapeutic approach for targeting this pathway.

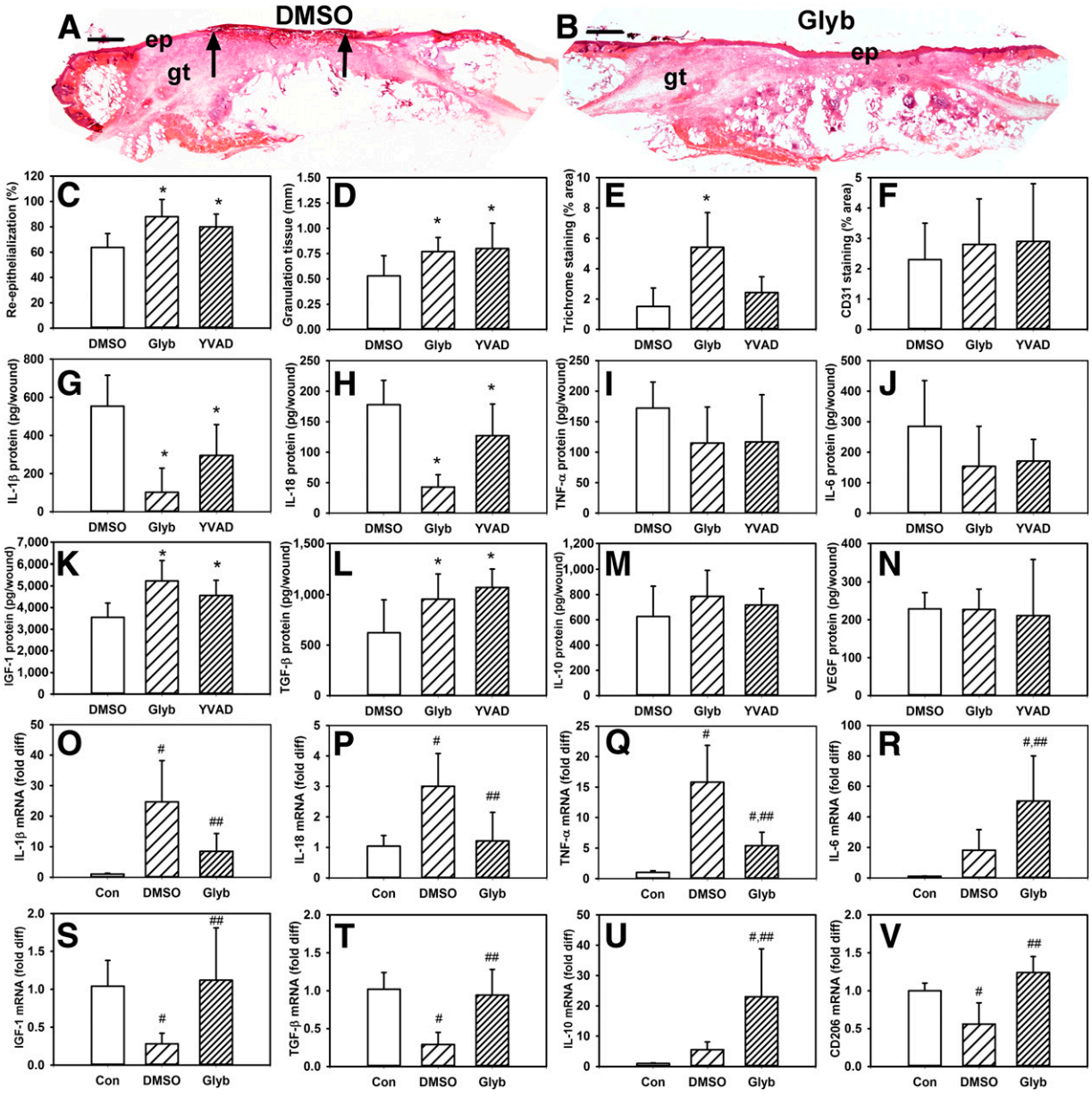


**Figure 6—**Blocking inflammasome activity downregulates the proinflammatory wound environment, upregulates a prohealing environment, and improves healing in diabetic mice. *A* and *B*: Excisional wounds in *db*/*db* mice whose wounds were treated topically with DMSO vehicle or glyburide (Glyb) harvested on day 10 postinjury, sectioned and stained with hematoxylin-eosin. Note the increased re-epithelialization in glyburide-treated wounds. ep, epithelium; gt, granulation tissue. Arrows indicate ends of epithelial tongues, scale bar = 0.5 mm. *C* and *D*: Re-epithelialization and granulation tissue thickness measured in hematoxylin-eosin–stained cryosections of wounds in *db*/*db* mice treated with DMSO, glyburide, or acYVAD-cmk (YVAD). Trichrome staining measured as pixels stained blue for collagen (*E*) and CD31 staining measured as pixels stained for this endothelial cell marker (*F*). *G*–*N*: Levels of cytokines in wound homogenates measured using ELISA, including proinflammatory cytokines IL-1β, IL-18, TNF-α, and IL-6 and healing-associated cytokines IGF-1, TGF-β, IL-10, and VEGF. *O*–*V*: Mp isolated from wounds in *db*/*db* mice treated with DMSO or glyburide and expression of proinflammatory cytokines IL-1β, IL-18, TNF-α, and IL-6 and healing-associated cytokines IGF-1, TGF-β, IL-10, and CD206 assessed by real-time PCR. For comparison, bone marrow–derived Mp from wild-type mice were left nonstimulated (Con) and gene expression was assessed along with wound Mp. For all graphs, bars = mean ± SD, $n$ = 6–8. Data compared between groups using ANOVA. *Mean value significantly different from that for DMSO-treated wounds; #mean value significantly different from that for nonstimulated in vitro control Mp; ##mean value significantly different from that for Mp isolated from DMSO-treated wounds; $P < 0.05$. Diff, difference.

Much has been learned recently about the pathways involved in activating the inflammasome; however, far less is known about the negative regulators that act as a brake on inflammasome activity. After activation signals, NLRP-3 monomers are thought to oligomerize and the caspase-1 adaptor protein ASC is recruited through pyrin domain interactions, and then caspase-1 is recruited to ASC through the caspase recruitment

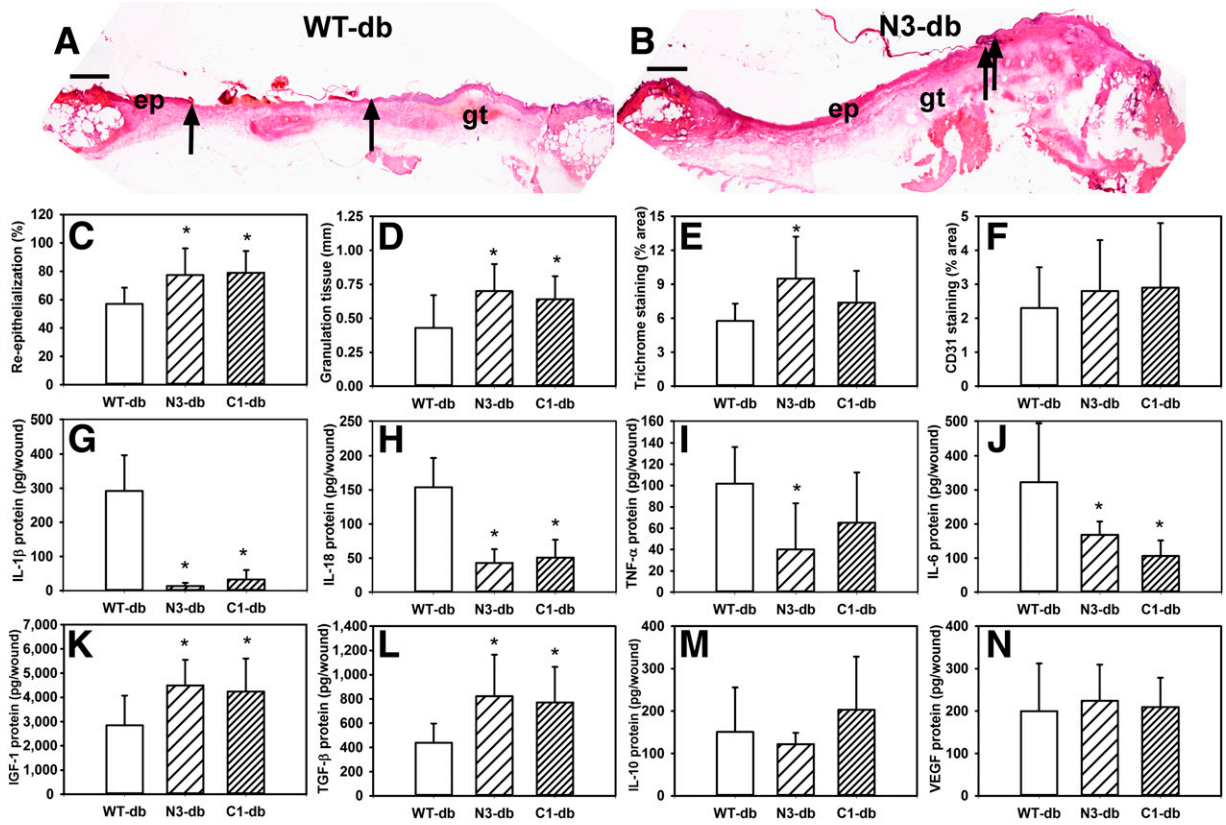


**Figure 7—** Bone marrow transfer from NLRP-3 and caspase-1–null mice to *db/db* mice is sufficient to downregulate the proinflammatory wound environment, upregulate a prohealing environment, and improve healing in diabetic mice. *A* and *B*: *db/db* Mice were subjected to lethal irradiation, and then bone marrow from wild-type (WT) or NLRP-3 (N3)–null mice was transferred 24 h later. Four weeks later, mice were subjected to excisional wounding, and wounds were harvested on day 10 postinjury, sectioned, and stained with hematoxylin-eosin. Note the increased re-epithelialization in *db/db* mice receiving NLRP-3 bone marrow. ep, epithelium; gt, granulation tissue. Arrows indicate ends of epithelial tongues, scale bar = 0.5 mm. *C* and *D*: Re-epithelialization and granulation tissue thickness measured in hematoxylin-eosin–stained cryosections of *db/db* mice receiving bone marrow from wild-type (WT-db) or NLRP-3–null (N3-db) or caspase-1–null (C1-db) mice. Trichrome staining measured as pixels stained blue for collagen (*E*) and CD31 staining measured as pixels stained for this endothelial cell marker (*F*). *G–N*: Levels of cytokines in wound homogenates measured using ELISA, including proinflammatory cytokines IL-1β, IL-18, TNF-α, and IL-6 and healing-associated cytokines IGF-1, TGF-β, IL-10, and VEGF. For all graphs, bars = mean ± SD, $n = 6–8$. Data compared between groups using ANOVA. *Mean value significantly different from that for mice receiving wild-type bone marrow; $P < 0.05$.

domain interactions. Caspase recruitment domain–only proteins (COPs), such as Iceberg, Pseudo-ICE, and caspase-12, and pyrin domain–only proteins (POPs), such as pyrin, POP1, and POP2, are thought to inhibit inflammasome activity by blocking inflammasome assembly and subsequent caspase-1 cleavage (16,39). In addition, other inhibitors such as PI-9 act by directly binding and inhibiting caspase-1 (40,41). Interestingly, humans express a broad array of COPs and POPs, whereas rodents only express a limited subset (16,39). We found that PI-9 and caspase-12 are upregulated in Mp as they switch from a proinflammatory to a prohealing phenotype in nondiabetic mice but that both the upregulation of these inflammasome inhibitors and the Mp phenotypic switch are impaired in diabetic mice. In addition, Mp isolated from chronic human diabetic wounds exhibited only low-level expression of PI-9 and caspase-12. Better understanding of the regulation of these inflammasome inhibitors may lead to additional targets for limiting inflammasome activity in inflammatory pathologies.

Components of the inflammasome can be expressed in cell types other than Mp that are involved in wound healing (42). For example, both murine and human keratinocytes express inflammasome components NLRP-3, ASC, caspase-1, IL-1β, and IL-18 (43,44). In addition, ultraviolet irradiation–induced IL-1β secretion from human keratinocytes in vitro appears to be mediated by the NLRP-3 inflammasome (43), and contact hypersensitivity appears to be mediated by the inflammasome/IL-1β pathway (44,45). Thus, topical application of glyburide and YVAD in our studies could block inflammasome activity in keratinocytes as well as Mp. However, our studies also indicate that Mp are the dominant producers of IL-1β in wounds of diabetic mice, and our bone marrow–transfer experiments indicate that loss of bone marrow cell–derived inflammasome activity is sufficient

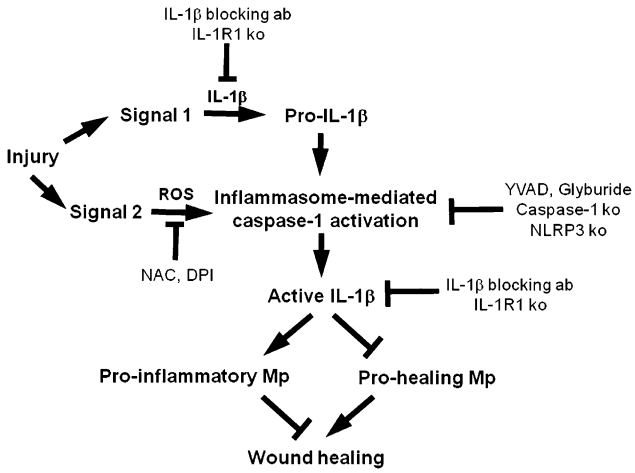


**Figure 8—**Model of the role of the inflammasome/IL-1β pathway in impaired wound healing in type 2 diabetes. Our data indicate that IL-1β can act as an upstream signal (signal 1) for sustaining inflammasome activity in chronic wound Mp and that ROS are involved in the second signal (signal 2) required for inflammasome activity. Since the inflammasome, in turn, activates IL-1β, this cytokine appears to be part of a proinflammatory positive-feedback loop that promotes a bias toward a proinflammatory Mp phenotype and inhibits upregulation of the prohealing phenotype and healing in diabetic wounds. ab, antibody; ko, knockout.

to reduce IL-1β and IL-18 levels in the wounds of diabetic mice. A limitation of our study is that the caspase-1–null mice were also found to be deficient in caspase-11 (46,47), and so our bone marrow–transfer experiments do not distinguish the role of these caspases in the impaired healing of wounds in *db/db* mice. Nonetheless, our experiments indicate that the NLRP-3 inflammasome plays an important role in the impaired healing of these wounds.

Accumulating evidence indicates that Mp are critical orchestrators in healing of many tissues, including skin (3,4,7,48). Recent studies have shown that Mp phenotypes change over the different phases of tissue repair and that the sequential appearance of these phenotypes may be required for efficient repair (11,14,29,49,50). In fact, either premature changes in phenotype or delayed/impaired changes in phenotype have been associated with impaired healing (14,29,49). Thus, further understanding of the regulation of the Mp phenotype, particularly in the setting of chronic wounds, could lead to improved therapeutic options for controlling inflammation in these wounds. Our data indicate that targeting the inflammasome may be an appealing candidate in this regard.

**Acknowledgments.** The authors thank Drs. Giamila Fantuzzi and Luisa DiPietro, University of Illinois at Chicago, for critical comments on a previous draft of the manuscript.

**Funding.** This study was supported by the National Institutes of Health (R01-GM-092850 to T.J.K.).

**Duality of Interest.** No potential conflicts of interest relevant to this article were reported.

**Author Contributions.** R.E.M. contributed to study design, researched data, and wrote the manuscript. M.M.F. and E.M.W.-H. researched data and reviewed and edited the manuscript. W.J.E. contributed to study design and reviewed and edited the manuscript. T.J.K. designed the study and wrote the manuscript. T.J.K. is the guarantor of this work and, as such, had full access to all the data in the study and takes responsibility for the integrity of the data and the accuracy of the data analysis.

**Prior Presentation.** Parts of this study were presented in abstract form at the Annual Meeting of the Wound Healing Society, Denver, CO, 1–5 May 2013.

## References

1. Singer AJ, Clark RA. Cutaneous wound healing. N Engl J Med 1999;341:738–746
2. Blakytny R, Jude E. The molecular biology of chronic wounds and delayed healing in diabetes. Diabet Med 2006;23:594–608
3. Arnold L, Henry A, Poron F, et al. Inflammatory monocytes recruited after skeletal muscle injury switch into antiinflammatory macrophages to support myogenesis. J Exp Med 2007;204:1057–1069
4. Mirza R, DiPietro LA, Koh TJ. Selective and specific macrophage ablation is detrimental to wound healing in mice. Am J Pathol 2009;175:2454–2462
5. Nahrendorf M, Swirski FK, Aikawa E, et al. The healing myocardium sequentially mobilizes two monocyte subsets with divergent and complementary functions. J Exp Med 2007;204:3037–3047
6. Ricardo SD, van Goor H, Eddy AA. Macrophage diversity in renal injury and repair. J Clin Invest 2008;118:3522–3530
7. Duffield JS, Forbes SJ, Constandinou CM, et al. Selective depletion of macrophages reveals distinct, opposing roles during liver injury and repair. J Clin Invest 2005;115:56–65
8. Goren I, Allmann N, Yogev N, et al. A transgenic mouse model of inducible macrophage depletion: effects of diphtheria toxin-driven lysozyme M-specific cell lineage ablation on wound inflammatory, angiogenic, and contractive processes. Am J Pathol 2009;175:132–147
9. Leibovich SJ, Ross R. The role of the macrophage in wound repair. A study with hydrocortisone and antimacrophage serum. Am J Pathol 1975;78:71–100
10. Lucas T, Waisman A, Ranjan R, et al. Differential roles of macrophages in diverse phases of skin repair. J Immunol 2010;184:3964–3977
11. Willenborg S, Lucas T, van Loo G, et al. CCR2 recruits an inflammatory macrophage subpopulation critical for angiogenesis in tissue repair. Blood 2012;120:613–625
12. Goren I, Kämpfer H, Podda M, Pfeilschifter J, Frank S. Leptin and wound inflammation in diabetic ob/ob mice: differential regulation of neutrophil and macrophage influx and a potential role for the scab as a sink for inflammatory cells and mediators. Diabetes 2003;52:2821–2832
13. Greenhalgh DG, Sprugel KH, Murray MJ, Ross R. PDGF and FGF stimulate wound healing in the genetically diabetic mouse. Am J Pathol 1990;136:1235–1246
14. Mirza R, Koh TJ. Dysregulation of monocyte/macrophage phenotype in wounds of diabetic mice. Cytokine 2011;56:256–264
15. Mirza RE, Fang MM, Ennis WJ, Koh TJ. Blocking IL-1β induces a healing-associated wound macrophage phenotype and improves healing in type 2 diabetes. Diabetes 2013;62:2579–2587
16. Martinon F, Mayor A, Tschopp J. The inflammasomes: guardians of the body. Annu Rev Immunol 2009;27:229–265

17. Strowig T, Henao-Mejia J, Elinav E, Flavell R. Inflammasomes in health and disease. Nature 2012;481:278–286
18. Pedra JH, Cassel SL, Sutterwala FS. Sensing pathogens and danger signals by the inflammasome. Curr Opin Immunol 2009;21:10–16
19. Mast BA, Schultz GS. Interactions of cytokines, growth factors, and proteases in acute and chronic wounds. Wound Repair Regen 1996;4:411–420
20. Trengove NJ, Stacey MC, MacAuley S, et al. Analysis of the acute and chronic wound environments: the role of proteases and their inhibitors. Wound Repair Regen 1999;7:442–452
21. Dinarello CA. Immunological and inflammatory functions of the interleukin-1 family. Annu Rev Immunol 2009;27:519–550
22. Wietecha MS, Chen L, Ranzer MJ, et al. Sprouty2 downregulates angiogenesis during mouse skin wound healing. Am J Physiol Heart Circ Physiol 2011;300:H459–H467
23. Barichello JM, Morishita M, Takayama K, Nagai T. Absorption of insulin from pluronic F-127 gels following subcutaneous administration in rats. Int J Pharm 1999;184:189–198
24. Bryer SC, Fantuzzi G, Van Rooijen N, Koh TJ. Urokinase-type plasminogen activator plays essential roles in macrophage chemotaxis and skeletal muscle regeneration. J Immunol 2008;180:1179–1188
25. Tschopp J, Schroder K. NLRP3 inflammasome activation: The convergence of multiple signalling pathways on ROS production? Nat Rev Immunol 2010;10:210–215
26. Loots MA, Lamme EN, Zeegelaar J, Mekkes JR, Bos JD, Middelkoop E. Differences in cellular infiltrate and extracellular matrix of chronic diabetic and venous ulcers versus acute wounds. J Invest Dermatol 1998;111:850–857
27. Rosner K, Ross C, Karlsmark T, Petersen AA, Gottrup F, Vejlsgaard GL. Immunohistochemical characterization of the cutaneous cellular infiltrate in different areas of chronic leg ulcers. APMIS 1995;103:293–299
28. Trengove NJ, Bielefeldt-Ohmann H, Stacey MC. Mitogenic activity and cytokine levels in non-healing and healing chronic leg ulcers. Wound Repair Regen 2000;8:13–25
29. Rodero MP, Hodgson SS, Hollier B, Combadiere C, Khosrotehrani K. Reduced Il17a expression distinguishes a Ly6c(lo)MHCII(hi) macrophage population promoting wound healing. J Invest Dermatol 2013;133:783–792
30. Sindrilaru A, Peters T, Wieschalka S, et al. An unrestrained proinflammatory M1 macrophage population induced by iron impairs wound healing in humans and mice. J Clin Invest 2011;121:985–997
31. Dinarello CA. Therapeutic strategies to reduce IL-1 activity in treating local and systemic inflammation. Curr Opin Pharmacol 2004;4:378–385
32. Larsen CM, Faulenbach M, Vaag A, et al. Interleukin-1-receptor antagonist in type 2 diabetes mellitus. N Engl J Med 2007;356:1517–1526
33. Osborn O, Brownell SE, Sanchez-Alavez M, Salomon D, Gram H, Bartfai T. Treatment with an Interleukin 1 beta antibody improves glycemic control in diet-induced obesity. Cytokine 2008;44:141–148
34. Stienstra R, van Diepen JA, Tack CJ, et al. Inflammasome is a central player in the induction of obesity and insulin resistance. Proc Natl Acad Sci USA 2011;108:15324–15329
35. Vandanmagsar B, Youm YH, Ravussin A, et al. The NLRP3 inflammasome instigates obesity-induced inflammation and insulin resistance. Nat Med 2011;17:179–188
36. Brem H, Kodra A, Golinko MS, et al. Mechanism of sustained release of vascular endothelial growth factor in accelerating experimental diabetic healing. J Invest Dermatol 2009;129:2275–2287
37. Hamed S, Ullmann Y, Masoud M, Hellou E, Khamaysi Z, Teot L. Topical erythropoietin promotes wound repair in diabetic rats. J Invest Dermatol 2010;130:287–294
38. Lamkanfi M, Mueller JL, Vitari AC, et al. Glyburide inhibits the Cryopyrin/Nalp3 inflammasome. J Cell Biol 2009;187:61–70
39. Stehlik C, Dorfleutner A. COPs and POPs: modulators of inflammasome activity. J Immunol 2007;179:7993–7998
40. Young JL, Sukhova GK, Foster D, Kisiel W, Libby P, Schönbeck U. The serpin proteinase inhibitor 9 is an endogenous inhibitor of interleukin 1beta-converting enzyme (caspase-1) activity in human vascular smooth muscle cells. J Exp Med 2000;191:1535–1544
41. Annand RR, Dahlen JR, Sprecher CA, et al. Caspase-1 (interleukin-1beta-converting enzyme) is inhibited by the human serpin analogue proteinase inhibitor 9. Biochem J 1999;342:655–665
42. Yazdi AS, Drexler SK, Tschopp J. The role of the inflammasome in non-myeloid cells. J Clin Immunol 2010;30:623–627
43. Feldmeyer L, Keller M, Niklaus G, Hohl D, Werner S, Beer HD. The inflammasome mediates UVB-induced activation and secretion of interleukin-1beta by keratinocytes. Curr Biol 2007;17:1140–1145
44. Watanabe H, Gaide O, Pétrilli V, et al. Activation of the IL-1beta-processing inflammasome is involved in contact hypersensitivity. J Invest Dermatol 2007;127:1956–1963
45. Sutterwala FS, Ogura Y, Szczepanik M, et al. Critical role for NALP3/CIAS1/Cryopyrin in innate and adaptive immunity through its regulation of caspase-1. Immunity 2006;24:317–327
46. Kayagaki N, Warming S, Lamkanfi M, et al. Non-canonical inflammasome activation targets caspase-11. Nature 2011;479:117–121
47. Broz P, Ruby T, Belhocine K, et al. Caspase-11 increases susceptibility to Salmonella infection in the absence of caspase-1. Nature 2012;490:288–291
48. van Amerongen MJ, Harmsen MC, van Rooijen N, Petersen AH, van Luyn MJ. Macrophage depletion impairs wound healing and increases left ventricular remodeling after myocardial injury in mice. Am J Pathol 2007;170:818–829
49. Perdiguero E, Sousa-Victor P, Ruiz-Bonilla V, et al. p38/MKP-1-regulated AKT coordinates macrophage transitions and resolution of inflammation during tissue repair. J Cell Biol 2011;195:307–322
50. Novak ML, Koh TJ. Macrophage phenotypes during tissue repair. J Leukoc Biol 2013;93:875–881